A Practical Stability Control Strategy for DC/DC Converters

Lin Jiang* and Po Li[†]

Abstract – This paper aims at designing an intelligent controller, based on control Lyapunov Function strategy integrated with fabricating discrete model of Buck and Boost converters and analyzing energy changes during the DC/DC progress to realize tracing reference current on Buck and Boost converters. In addition, practical stability phenomenon research and transient performance analysis has been proposed to give an insight to the influence of controller parameters in achieving an enhanced output performance and how the time of sample period affect the error of practical stability will be illustrated. The novelty of this controller in comparison to other schemes lies in the improved performance of practical stability.

Keywords: Practical stability, Discrete lyapunov function, Finite input set.

1. Introduction

In recent years, DC/DC converters are widely used in automotive, electronics, electrical appliances, aerospace, new energy, IT and medical facilities, especially in renewable system. Improving the stability and proficiency of DC/DC converters can accelerate the development of photovoltaic and wind energy, which has been widely studied around the world [1]. By matching the voltage between various energy sources, most applications require DC/DC converters in order to achieve energy output and recovery [2]. Nowadays, by the development of power electronics and microelectronics, the market demands strict limits on their size and weight, together with high performance and efficiency, so DC/DC converters must update constantly, and their control strategies also need to advance all the time, especially in their tracking performances and robustness. Searching for adequate control mechanism for Buck and Boost converters has drawn attention of the research community in order to gain more insight into the aspects of controller design and stability issues, thereby contributing to the improvements in transient and steady state behavior under the influence of different disturbances.

Conventional proportional-integral-derivative (PID) controllers which involves linearizing the converter around a specific operating point [3], and finding the gain parameters of the controller based on the concepts of linear control theory are still one of the most commonly used control methods for converters by far. Paper [4] has used integral method, which has been widely used in studying stability research in DC/DC converters, to investigate the steady state performance. However, this method need to set the time of differential and integral periods based on average tracing current and construct average mathematic models, so the PID control systems suffer from the limitations of slow compensator and hysteresis, which lead to poor dynamic performances of converters in most cases. In other words, PID control method cannot ensure robustness over a wide range of operating points [5]. Sliding mode control(SMC) [6-8] which is another method widely used in converters, is a kind of non-linear strategy which gained popularity due to its immunity towards parameters uncertainties, its simple structure and dis-continuous switching control signals which makes it a good choice for applications in power converters. However, when the converter is subjected to a wide range of mismatched uncertainties, the SMC method cannot assure robustness of converters. Back stepping control [9] is another important non-linear control technique applicable to systems in the strict feedback form. The features include a systematic framework for the controller design, ease of understanding and implementation and can successfully reject both linearly parameterized matched and mismatched uncertainties. However, since the computation of the control signal demands the exact knowledge of system parameters at any instant of time, which may not be available, hence it is not an attractive choice for control applications. In [10] fuzzy control with integral action for pulse width modulation (PWM) DC/DC converter is presented, which is a novel control method for converters based on intelligence algorithms. Such methods are found to exhibit near satisfactory transient and steady state performance. Besides, using fuzzy control and other intelligence methods can reduce the calculation in some respects. However, this area is still under investigation for further improvements as regards to the control dynamics. In addition, some researches concentrate on stability

† Corresponding Author: Department of Instrumental Electrical Engineering, School of Aerospace Engineering, Xiamen University 361005, China; Shenzhen Research Institute of Xiamen University 518063, China. (lipo@xmu.edu.cn)
* Department of Instrumental Electrical Engineering, School of Aerospace Engineering, Xiamen University 361005, China; Shenzhen Research Institute of Xiamen University 518063, China. (jianglin@stu.xmu.edu.cn)

studies of sophisticated converters models lately including buck-boost models, Cuk models, combination of traditional converters and so on. Paper [11] has shown steady research on Quasi-Cuk DC/DC converter with reduced voltage stress on capacitor.

The objective of this paper is to design an intelligent controller, based on control Lyapunov Function strategy integrated with fabricating discrete model of Buck and Boost converters and analyzing energy changes during the DC/DC progress to realize tracing reference current on Buck and Boost converters. In addition, practical stability phenomena research and transient performance analysis has been proposed to give an insight to the influence of controller parameters in achieving an enhanced output performance and how the time of sample period affect the error of practical stability will be illustrated. The novelty of this controller in comparison to other schemes lies in the improved performance of practical stability. Further an attempt to utilize discrete energy function to fabricate the 3D field of the differential of control Lyapunov Function has also been made in order to analysis the tracing progress which highlights the significant merit in the proposed control method.

2. Model Description for Buck Converter

Fig. 1 shows a typical model for DC/DC Buck converter circuit, where i_L and v_c represent the inductor current and the output capacitor voltage respectively, R is the load resistance of the circuit, and U is a DC input voltage source. The system model for DC/DC Buck converter can be written as follows:

$$\begin{cases} \dfrac{di_L}{dt} = \dfrac{1}{L}(U - v_c) \\ \dfrac{dv_c}{dt} = \dfrac{1}{C}(i_L - \dfrac{v_c}{R}) \end{cases} \text{(Switch T is on)} \quad (1)$$

$$\begin{cases} \dfrac{di_L}{dt} = -\dfrac{1}{L}v_c \\ \dfrac{dv_c}{dt} = \dfrac{1}{C}(i_L - \dfrac{v_c}{R}) \end{cases} \text{(Switch T is off)} \quad (2)$$
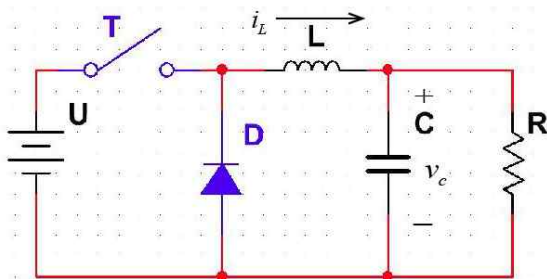

Fig. 1. a typical model for DC/DC Buck converter circuit

Integrating formula 1 and 2 and introducing S to represent the state of switch (S=1 or 0 represents that switch T is on or off respectively), the switching model of Buck converter can be expressed as follow:

$$\begin{cases} \dfrac{di_L}{dt} = \dfrac{1}{L}(US - v_c) \\ \dfrac{dv_c}{dt} = \dfrac{1}{C}(i_L - \dfrac{v_c}{R}) \end{cases} \quad (3)$$

Where S has finite input 0 or 1. The observer model is designed by copying the switch model and introducing symbol * to represent observational parameters of model for acquiring values of i_L and v_c:

$$\begin{cases} \dfrac{di_L^*}{dt} = \dfrac{1}{L}(US^* - v_c^*) \\ \dfrac{dv_c^*}{dt} = \dfrac{1}{C}(i_L^* - \dfrac{v_c^*}{R}) \end{cases} \quad (4)$$

Making a subtraction between 3 and 4. Meanwhile, in order to show the functions more directly and clearly, this paper use x_1 to represent i_L and x_2 to represent v_c. The error model of DC/DC Buck converter circuit can be expressed as follow:

$$\begin{cases} \dfrac{d\widetilde{x_1}}{dt} = \dfrac{1}{L}[U(S - S^*) - \widetilde{x_2}] \\ \dfrac{d\widetilde{x_2}}{dt} = \dfrac{1}{C}(\widetilde{x_1} - \dfrac{\widetilde{x_2}}{R}) \end{cases} \quad (5)$$

where $\widetilde{x_1} = x_1 - x_1^*$, $\widetilde{x_2} = x_2 - x_2^*$, $S - S^* \in \{0 - S^*, 1 - S^*\}$ and $S^* \in [0,1]$.

Selecting positive function $V = \dfrac{1}{2}L\widetilde{x_1}^2 + \dfrac{1}{2}C\widetilde{x_2}^2$ as Lyapunov Function for continuous states, the derivative of V can demonstrate as follow:

$$\dot{V} = [U(S - S^*) - \widetilde{x_2}]\widetilde{x_1} + \widetilde{x_2}(\widetilde{x_1} - \dfrac{\widetilde{x_2}}{R}) = U(S - S^*)\widetilde{x_1} - \dfrac{\widetilde{x_2}^2}{R}$$

As long as designing a control strategy to make $S - S^*$ and $\widetilde{x_1}$ have opposite sign at any time, $\dot{V} \leq 0$ will be accomplished. Selecting appropriate input state (S=1 or 0), demands have been mentioned above can be accomplished easily.

Taking control period is limited into consideration, discrete model will be accomplished by using discretization method for formula 5. Introducing $\widetilde{S}$ to represent $S - S^*$; $(k+1)$ and (k) represent the time of $k+1$ and k respectively and T_s represents the sample time. Discretization of formula 5 can be express as follow:

$$\begin{cases} \widetilde{x_1}(k+1) = \dfrac{T_s}{L}U\widetilde{S}(k) - \dfrac{T_s}{L}\widetilde{x_2}(k) + \widetilde{x_1}(k) \\ \widetilde{x_2}(k+1) = \dfrac{T_s}{C}\widetilde{x_1}(k) - \dfrac{T_s}{RC}\widetilde{x_2}(k) + \widetilde{x_2}(k) \end{cases} \quad (6)$$

Utilizing function $V(k)=\dfrac{1}{2}\big[L\widetilde{x_1}(k)\big]^2+\dfrac{1}{2}\big[C\widetilde{x_2}(k)\big]^2$ to describe the process of stabilization.

$$\begin{aligned} \Delta V &= V(k+1)-V(k) \\ &= \tfrac{1}{2}L\widetilde{x_1}(k+1)^2+\tfrac{1}{2}C\widetilde{x_2}(k+1)^2-\tfrac{1}{2}L\widetilde{x_1}(k)^2-\tfrac{1}{2}C\widetilde{x_2}(k)^2 \\ &= \dfrac{T_s^2}{2L}\big[U\widetilde{S}(k)-\widetilde{x_2}(k)\big]^2+\dfrac{T_s^2}{2C}\Big[\widetilde{x_1}(k)-\dfrac{\widetilde{x_2}(k)}{R}\Big]^2 \\ &\quad + T_s U\widetilde{S}(k)\widetilde{x_1}(k)-\dfrac{T_s}{R}\widetilde{x_2}(k)^2 \end{aligned} \quad (7)$$

Function 7 is sophisticated, however, the polynomial $T_s U\widetilde{S}(k)\widetilde{x_1}(k)$ could be controlled negatively by selecting the state of $S-S^*$ and $\widetilde{x_1}$ have opposite sign at any time. Besides, if we make T_s is short enough, polynomial $\dfrac{T_s^2}{2L}\big[U\widetilde{S}(k)-\widetilde{x_2}(k)\big]^2+\dfrac{T_s^2}{2C}\Big[\widetilde{x_1}(k)-\dfrac{\widetilde{x_2}(k)}{R}\Big]^2$ could not affect the negative of function intensely. Thus, if we select suitable sample time, the negative of discrete Lyapunov Function can be realized by controlling the switch in Buck converter. However, switch state cannot change during one control period which leads to the state of $\Delta V>0$ may maintain in a very short time less than the time of one period if the ideal moment of changing switch state occurs during the control period. It means stability area has replaced the stable point as the ideal control targets based on practical stability control strategy.

In order to investigate the practical stability under the control strategy of $\Delta V<0$, this paper researched on the cross section under $\Delta V=0$ in Fig. 2.
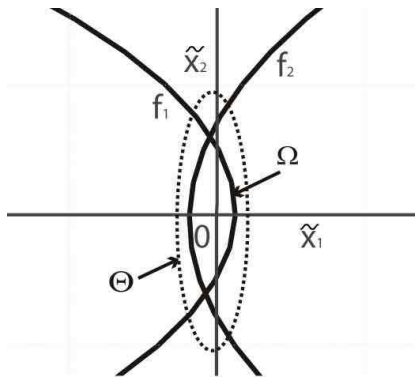

Fig. 2. $\Delta V=0$ plane under situations of $S=1or0$

Defining $\Delta V=f_1$ when $S=0$ and $\Delta V=f_2$ when $S=1$. On the left of line f_1, $f_1>0$; On the right of line f_1, $f_1<0$. Similarly, On the right of line f_2, $f_2>0$; On the left of line f_2, $f_2<0$. Supposing the max energy of $\Delta V=0$ encircles the area Ω equals E_Ω and the max changes of energy during one control period is ΔE_T, so the max energy of work situation after the first entering into the area Ω is $E_\Omega+\Delta E_T$. In other words, we can find an area Θ determined by $E_\Omega+\Delta E_T$ where the work situation cannot escape from when entering this area. If increasing the value of control frequency, the size of Θ can be decreased; and if the control frequency is limitless, these states will be as same as the states under continuous control to accomplish asymptotic stability which is the same as the conclusion under continuous researches.

3. Model Description for Boost Converter

Discrete model designing for Boost converter is similar to the Buck converter, except for the next two points: 1. The relation between states of switch and energy of circuit is different from Buck converter; 2. Nonlinear product term will influence the size of uncontrollable area. Fig. 3 shows a typical DC/DC Boost converter circuit, where i_L is the inductor current, and v_c represents the output capacitor voltage. R is the load resistance of the circuit, and U is a dc input voltage source. The system model for DC/DC Boost converter can be written as follows:

$$\begin{cases} \dfrac{di_L}{dt}=\dfrac{1}{L}U \\ \dfrac{dv_c}{dt}=-\dfrac{v_c}{CR} \end{cases} \text{(Switch T is on)} \quad (8)$$

$$\begin{cases} \dfrac{di_L}{dt}=\dfrac{1}{L}(U-v_c) \\ \dfrac{dv_c}{dt}=\dfrac{1}{C}(i_L-\dfrac{v_c}{R}) \end{cases} \text{(Switch T is off)} \quad (9)$$

Integrating formula 8 and 9 and introducing S to represent the state of switch (D=1or 0 represents that switch is on or off respectively), the switch model of Boost converter is able to express as follow:
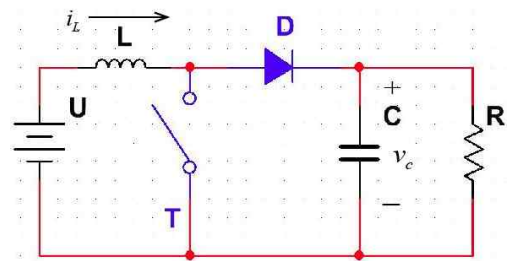

Fig. 3. a typical DC/DC Boost converter circuit

$$\begin{cases} \dfrac{di_L}{dt} = \dfrac{1}{L}(U - v_c(1-D)) \\ \dfrac{dv_c}{dt} = \dfrac{1}{C}(i_L(1-D) - \dfrac{v_c}{R}) \end{cases} \quad (10)$$

where D has finite input 0 or 1. The observer model is designed by copying the switch model and introducing symbol * to represent observational parameters of model for acquiring the i_L and v_c.

$$\begin{cases} 0 = \dfrac{di_L^*}{dt} = \dfrac{1}{L}(U - v_c^*(1-D^*)) \\ 0 = \dfrac{dv_c^*}{dt} = \dfrac{1}{C}(i_L^*(1-D^*) - \dfrac{v_c^*}{R}) \end{cases} \quad (11)$$

Making a subtraction between 3 and 4. Meanwhile, in order to show the functions more directly and clearly, this paper use x_1 and x_2 to represent i_L and v_c respectively.

$$\begin{cases} \dfrac{d\widetilde{x_1}}{dt} = \dfrac{1}{L}[U(S-S^*) - \widetilde{x_2}] \\ \dfrac{d\widetilde{x_2}}{dt} = \dfrac{1}{C}(\widetilde{x_1} - \dfrac{\widetilde{x_2}}{R}) \end{cases} \quad (12)$$

where $\widetilde{x_1} = x_1 - x_1^*$, $\widetilde{x_2} = x_2 - x_2^*$, $S - S^* \in \{0 - S^*, 1 - S^*\}$ and $S^* \in [0,1]$.

Selecting positive function $V = \dfrac{1}{2}L\widetilde{x_1}^2 + \dfrac{1}{2}C\widetilde{x_2}^2$ as continuous Lyapunov Function, the derivative of V can demonstrate as follow:

$$\begin{aligned} \dot{V} &= -[\widetilde{x_2}\widetilde{S} + x_2^*\widetilde{S} + \widetilde{x_2}S^*]\widetilde{x_1} + \widetilde{x_2}(\widetilde{x_1}\widetilde{S} + x_1^*\widetilde{S} + \widetilde{x_1}S^* - \dfrac{\widetilde{x_2}}{R}) \\ &= -\widetilde{x_1}x_2^*\widetilde{S} + \widetilde{x_2}x_1^*\widetilde{S} - \dfrac{\widetilde{x_2}^2}{R} \end{aligned}$$

For $S - S^*$ is nonpositive or nonnegative at any time, as long as designing a control strategy to make $S - S^*$ and $-\widetilde{x_1}x_2^* + \widetilde{x_2}x_1^*$ have opposite sign or the product of them is zero at any time, $\dot{V} \le 0$ will be accomplished.

Introducing $\widetilde{S}$ to represent $S - S^*$; $(k+1)$ and (k) represent the time of $k+1$ and k respectively and T_s represents the sample time. Discretization of formula 5 can be express as follow:

$$\begin{cases} \widetilde{x_1}(k+1) = \dfrac{T_s}{L}U\widetilde{S}(k) - \dfrac{T_s}{L}\widetilde{x_2}(k) + \widetilde{x_1}(k) \\ \widetilde{x_2}(k+1) = \dfrac{T_s}{C}\widetilde{x_1}(k) - \dfrac{T_s}{RC}\widetilde{x_2}(k) + \widetilde{x_2}(k) \end{cases} \quad (13)$$

Utilizing function $V(k) = \dfrac{1}{2}\left[L\widetilde{x_1}(k)\right]^2 + \dfrac{1}{2}\left[C\widetilde{x_2}(k)\right]^2$
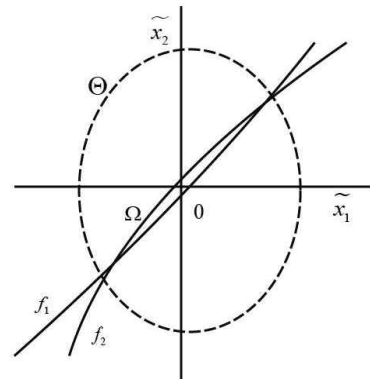

Fig. 4. $\Delta V = 0$ plane under situations of $S = 1$ or 0

to describe the process of stabilization.

$$\begin{aligned} \Delta V(k) &= V(k+1) - V(k) = \dfrac{1}{2}L\widetilde{x_1}(k+1)^2 \\ &+ \dfrac{1}{2}C\widetilde{x_2}(k+1)^2 - \dfrac{1}{2}L\widetilde{x_1}(k)^2 - \dfrac{1}{2}C\widetilde{x_2}(k)^2 \\ &= \dfrac{T_s^2}{2L}\left[-\widetilde{x_2}(k)\widetilde{S}(k) - x_2^*\widetilde{S}(k) - \widetilde{x_2}(k)S^*\right]^2 \\ &+ \dfrac{T_s^2}{2C}\left[\widetilde{x_1}(k)\widetilde{S}(k) + x_1^*\widetilde{S}(k) + \widetilde{x_1}(k)S^* - \dfrac{\widetilde{x_2}(k)}{R}\right]^2 \\ &- T_s x_2^*\widetilde{S}(k)\widetilde{x_1}(k) + T_s x_1^*\widetilde{S}(k)\widetilde{x_2}(k) - \dfrac{T_s}{R}\widetilde{x_2}(k)^2 \end{aligned} \quad (14)$$

Fig. 4 shows the $\Delta V = 0$ states under discrete control based on control Lyapunov Function.

Defining $\Delta V = f_1$ when $S = 0$ and $\Delta V = f_2$ when $S = 1$. On the left of line f_1, $f_1 > 0$; On the right of line f_1, $f_1 < 0$. Similarly, On the right of line f_2, $f_2 > 0$; On the left of line f_2, $f_2 < 0$. Supposing the max energy of $\Delta V = 0$ encircles the area Ω equals E_Ω and the max changes of energy during one control period is ΔE_T, so the max energy of work situation after the first entering into the area Ω is $E_\Omega + \Delta E_T$. In other words, we can find an area Θ which is similar to the buck converter control determined by $E_\Omega + \Delta E_T$ where the work situation cannot escape from when entering this area.

4. Simulations and Experiments for Buck Converter

Simulation parameters are listed in Table 1

Table 1. Simulation parameters

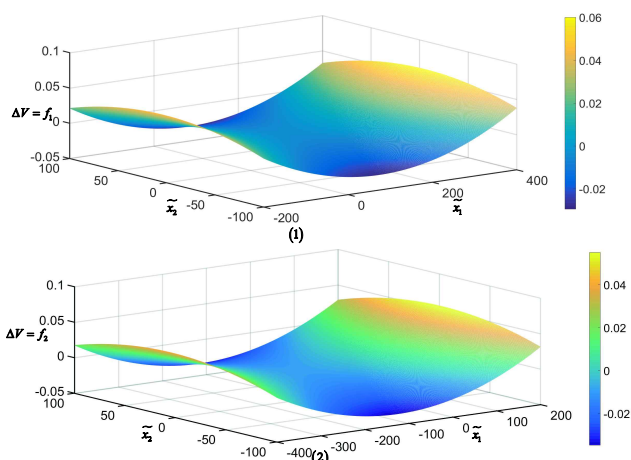|	
R(Ω)	20
L(H)	0.05
C(F)	0.002
U(V)	5
Control Frequency(kHz)	20

Fig. 5. (1) 3-D diagram of $\Delta V = f_1$; (2) 3-D diagram of $\Delta V = f_2$
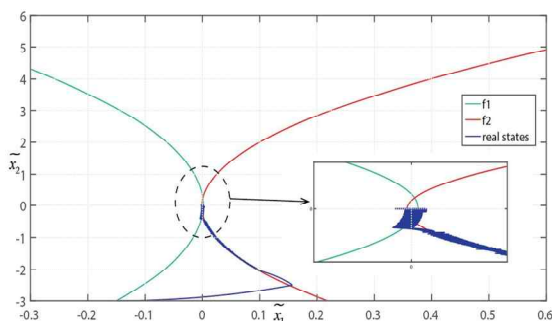

Fig. 6. Simulation of $\Delta V = 0$ plane with the real states during the control process

In Fig. 5 and Fig. 6, practical stability has been accomplished under the advanced control strategy and the real work situation cannot escape from an area when entering this area which is greater than the cross area slightly.

According to former researches, switch state cannot change during one control period which leads to the state of $\Delta V > 0$ may maintain in a very short time less than the time of one period if the ideal moment of changing switch state occurs during the control period. State $\Delta V > 0$ brings ΔE_T and the length of $\Delta V < 0$ time will influence the size of ΔE_T. Meanwhile,

$$T_s = \frac{2\widetilde{x_2}(k)^2 - 2U\widetilde{S}(k)\widetilde{x_1}(k)R}{\frac{R}{L}\left[U\widetilde{S}(k) - \widetilde{x_2}(k)\right]^2 + \frac{R}{C}\left[\widetilde{x_1}(k) - \frac{\widetilde{x_2}(k)}{R}\right]^2}$$

when $\Delta V = 0$ ($\Delta V = 0$ cannot cross the (0,0), so the denominator cannot equal to zero) according to function (7). It means control period has effects on the size of Ω area and E_Ω. Supposing an error function by energy function as follow in order to investigate the relations between time of control period and the area of practical stability:
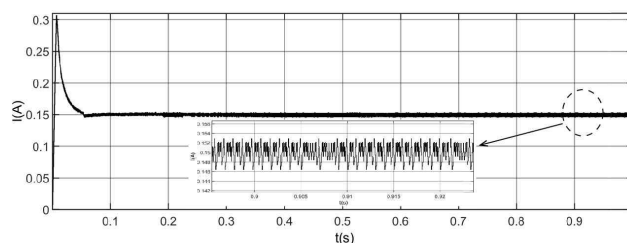
Fig. 7. Current tracing under the situations of $S^*=0.6$ and $i_L^* = 0.15A$ based on practical stability control strategy (unit of t-axis is s and unit of i_L-axis is A)
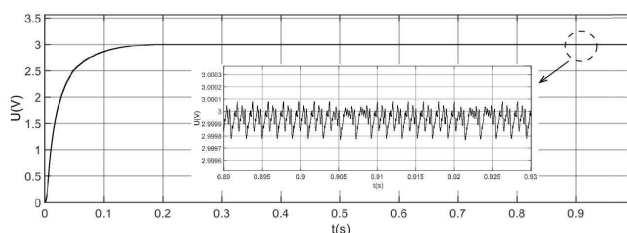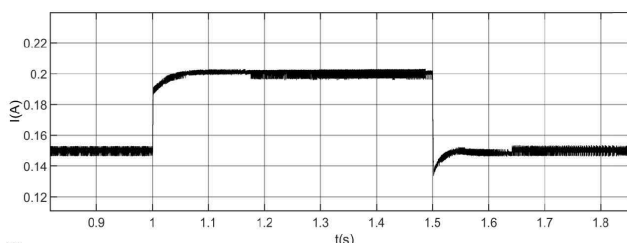

Fig. 8. Voltage tracing under the situations of $S^*=0.6$ and $i_L^* = 0.15A$ based on practical stability control strategy (unit of t-axis is s and unit of i_L-axis is A)

Fig. 9. Current tracing under the situations of $S^*=0.6$ and $i_L^* = 0.15A$ except 1s to 1.5s ($i_L^* = 0.2A$) (unit of t-axis is s and unit of i_L-axis is A)

$$J = \frac{1}{2}L\widetilde{x_1}^2 + \frac{1}{2}C\widetilde{x_2}^2$$

Table 2 and Fig. 10 shows the relationships between max J when the line of real states passes through the lines of $\Delta V = 0$ back and forth constantly and the control frequency. As we have noticed, the error is negative correlation to the control frequency. And, more remarkable, if we improve the control strategy after 10kHz the error performance will improve little under these simulation parameters listed in Table 1. Thus, this paper selects 10kHz as control strategy is suitable and effective.

Furthermore, this paper built CompactRIO 9073-FPGA experiments system to prove the control strategy for Buck converter as shown in Fig. 11. Table 3 demonstrates the experiments parameters and Fig. 12 and Fig. 13 shows the tracing results of control strategy.

Table 2. Relations between time of control period and max offset between energy function and reference parameters

kHz	10^-8J
200	1.9999
100	7.9995
50	25.951
40	38.871
20	148.89
10	591.47

Table 3. Experiments parameters

R(Ω)	4
L(H)	0.003
C(F)	0.00033
U(V)	12
Control Frequency(kHz)	**20**
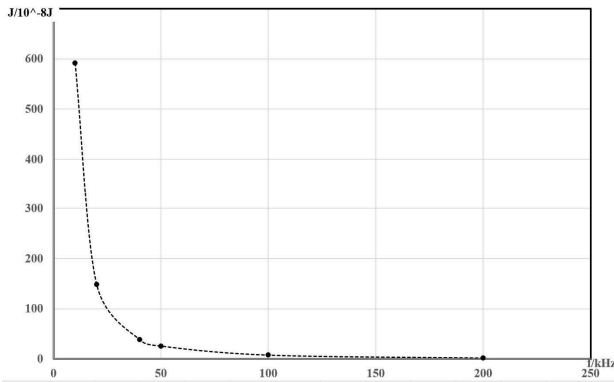
Fig. 10. Relations between time of control period and max offset between energy function and reference parameters

Fig. 11. Experimental platform based on NI CompactRIO 9073 FPGA

5. Simulations and Experiments for Boost Converter

Simulation parameters are listed in Table 4

Table 4. Simulation parameters

R(Ω)	20
L(H)	0.004
C(F)	0.002
U(V)	5
Control Frequency(kHz)	20
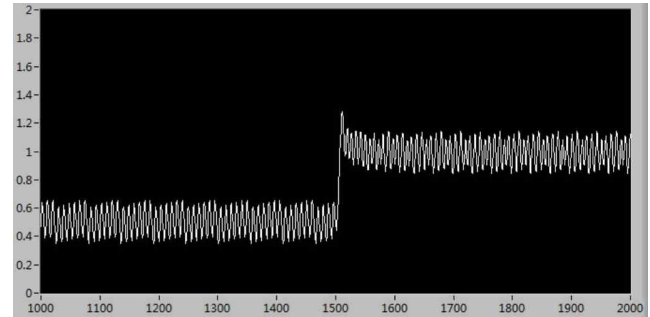
Fig. 12. Current tracing under the situations $u_c^* = 2V to 4V$ based on practical stability control strategy (unit of t-axis is 0.00005s and unit of i_L-axis is A)
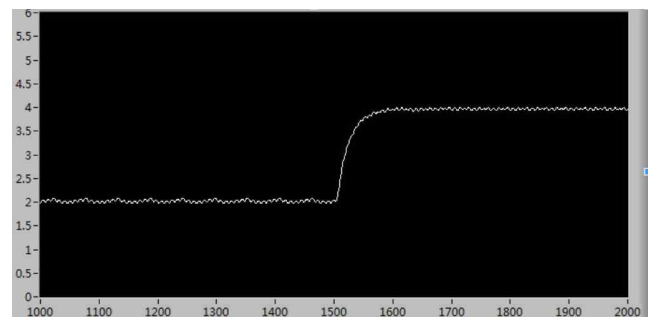
Fig. 13. Voltage tracing under the situations $u_c^* = 2V to 4V$ based on practical stability control strategy (unit of t-axis is 0.00005s and unit of u_c-axis is V)
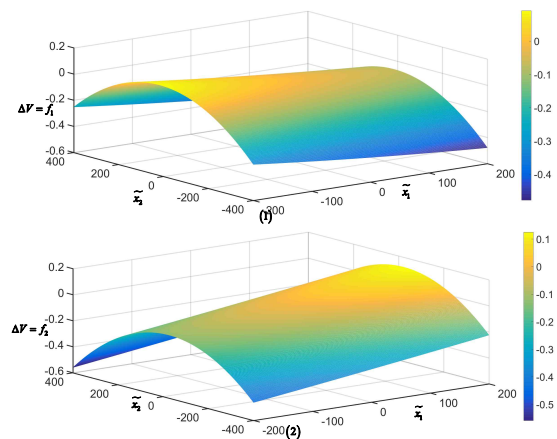

Fig. 14. (1) 3-D diagram of $\Delta V = f_1$; (2) 3-D diagram of $\Delta V = f_2$;
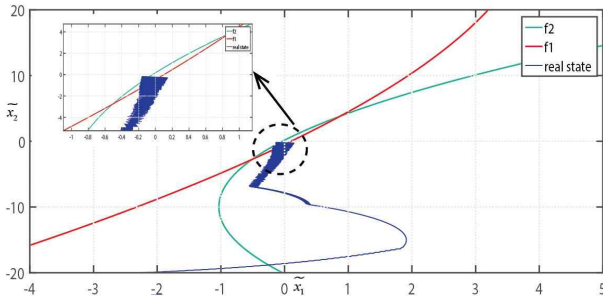
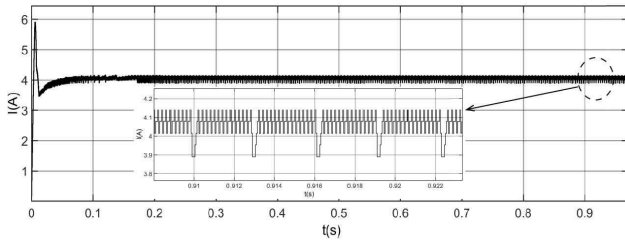**Fig. 15.** Simulation of $\Delta V = 0$ plane with the real states during the control process

Fig.16. Current tracing under the situations $u_c^* = 20V$ based on practical stability control strategy (unit of t-axis is s and unit of i_L-axis is A)
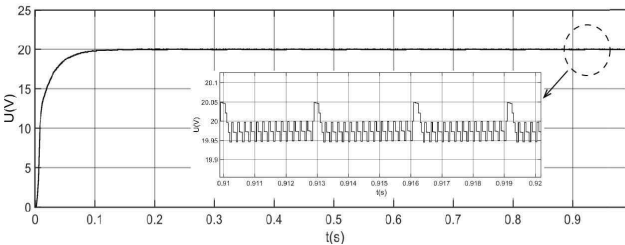

Fig.17. Voltage tracing under the situations $u_c^* = 20V$ based on practical stability control strategy (unit of t-axis is s and unit of i_L-axis is A)
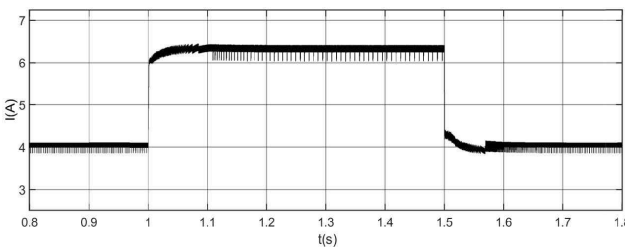

Fig. 18. Current tracing under the situations of $u_c^* = 20V$ except 1s to 1.5s ($u_c^* = 25V$)(unit of t-axis is s and unit of i_L-axis is A)

In Fig. 14 and Fig. 15, practical stability has been accomplished under the advanced control strategy and the real work situation cannot escape from an area when entering this area which is greater than the cross area slightly.

Table 5. Relations between time of control period and max offset between energy function and reference parameters

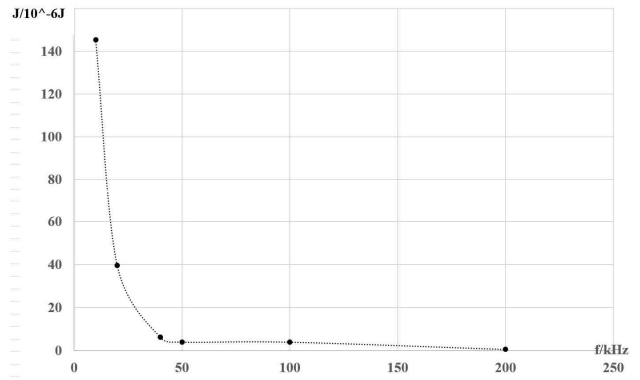| kHz	10^-6J
200	0.58086
100	3.9606
50	4.0015
40	6.2168
20	39.606
10	145.42

Fig. 19. Relations between time of control period and max offset between energy function and reference parameters

Supposing an error function by energy function as follow in order to investigate the relations between time of control period and the area of practical stability:

$$J = \frac{1}{2}L\widetilde{x_1}^2 + \frac{1}{2}C\widetilde{x_2}^2$$

Table 5 and Fig. 16 shows the relationships between max J when the line of real states passes through the lines of $\Delta V = 0$ back and forth constantly and the control frequency. As we have noticed, the error is negative correlation to the control frequency. And, more remarkable, if we improve the control strategy after 10kHz the error performance will improve little under these simulation parameters listed in Table 1. Thus, this paper selects 20kHz as control strategy is suitable and effective.

Furthermore, this paper build CompactRIO 9073-FPGA experiments system to prove the control strategy for Boost converter as shown in Fig. 11. Table 6 demonstrates the experiments parameters and Fig. 20 and Fig. 21 shows the tracing results of control strategy.

Table 6. Experiments parameters

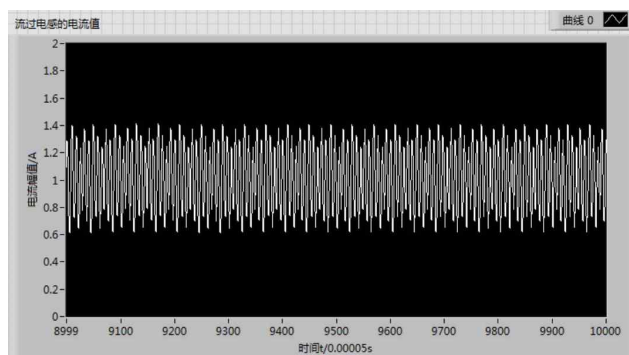| R(Ω)	50
L(H)	0.003
C(F)	0.00033
U(V)	12
Control Frequency(kHz)	**20**

Fig. 20. Current tracing under the situations $u_c^* = 24V$ based on practical stability control strategy (unit of t-axis is 0.00005s and unit of u_c-axis is V)
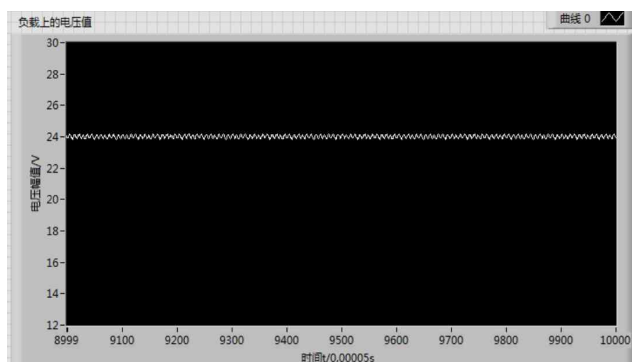

Fig. 21. Voltage tracing under the situations $u_c^* = 24V$ based on practical stability control strategy (unit of t-axis is 0.00005s and unit of u_c-axis is V)

6. Conclusion

In this study, the stability characteristics of DC/DC converter were investigated, and a control strategy based on discrete Lyapunov Function was developed to obtain the practical stability of DC/DC converter.

In order to investigate the sophisticated process, 3-D diagram about the change of energy was generated. According to simulation, the following conclusions were obtained.

(1) Due to the finite input set, practical stability can be realized in DC/DC converter via selecting suitable sample time and controlling the switch under the control strategy demonstrated by discrete Lyapunov Function.

(2) To investigate the energy changes during the work time of DC/DC converter, we could find a finite stable area which contains all current and voltage situations when the S^* is chosen.

(3) Sample time affects the finite stable area intensely. If we could improve the sample time as more as possible, the finite stable area will become smaller.

References

[1] Chang-Soon Lim and Kui-Jun Lee, "Nonisolated Two-Phase Bidirectional DC-DC Converter with Zero-Voltage-Transition for Battery Energy Storage System," *in J Electr Eng Technol.*, vol. 12, no. 6, pp. 2237-2246, 2017.

[2] Luo Yutao and Wang Feng, "Optimization of Bidirectional DC/DC Converter for Electric Vehicles Based on Driving Cycle," *in J Electr Eng Technol.*, vol. 12, no. 5, pp. 1934-1944, 2017.

[3] H. Sira-Ramirez, "Nonlinear P-I controller design for switch mode DC-to-DC power converters," *IEEE Trans. Circuits Syst.*, vol. 38, no. 4, pp. 410-417, 1991.

[4] Divya Navamani. J, Vijayakumar. K, Jegatheesan. R and Lavanya. A, "High Step-up DC-DC Converter by Switched Inductor and Voltage Multiplier Cell for Automotive Applications," *in J Electr Eng Technol.*, vol. 12, no. 1, pp. 189-197, 2017.

[5] A. Soto, P. Alou, J. A. Oliver, J. A. Cobos, and J. Uceda, "Optimum control design of PWM-buck topologies to minimize output impedance," *in Proc. 17th Annu. IEEE Appl. Power Electron. Conf. Expo. (APEC)*, pp. 426-432, Mar. 2002.

[6] V.I. Utkin, "Variable structure systems with sliding modes," *IEEE Trans. Autom. Control*, vol. 22, no. 2, pp. 212-222, 1977.

[7] C. Edwards, S. K. Spurgeon, "Sliding Mode Control: Theory and Applications, Taylor & Francis, Francis," London, UK, 1998.

[8] Vadim Utkin, "Sliding mode control of DC/DC converters," *J. Frankl. Inst.*, vol. 350, no. 8, pp. 2146-2165, 2013.

[9] Shui-Chun Lin, Ching-Chin Tsai, "Adaptive back stepping control with integral action for PWM buck DC-DC converters," *J. Chin. Inst. Eng.*, vol. 28, no. 6, pp. 977-984, 2005.

[10] Marikkannan. A and Manikandan. B.V, "Fuzzy Controlled ZVS Asymmetrical PWM Full-bridge DC-DC Converter for Constant Load High Power Applications," *in J Electr Eng Technol.*, vol. 12, no. 3, pp. 1235-1244, 2017.

[11] Elias Shokati Asl and Mehran Sabahi, "Bidirectional Quasi-Cuk DC/DC Converter with Reduced Voltage Stress on Capacitor and Capability of Changing the Output Polarity," *in J Electr Eng Technol.*, vol. 12, no. 3, pp. 1108-1113, 2017.
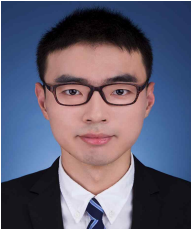
Lin Jiang He received his B.S. degree in Department of Mechanical and Electrical Engineering and his M.S. degree in Department of Instrumental Electrical Engineering from Xiamen University, Xiamen, China, in 2014 and 2017. His research interests include control strategy and power electronics.

Po Li He received the B.S. degree in electronics information engineering and Ph.D. degree in electrical and electronics engineering from Wuhan University, Wuhan, China, in 2004 and 2010 respectively. From 2006 to 2010, He was a co-researcher in control engineering in Sophia University, Tokyo, Japan. He is currently an Assistant Professor with Xiamen University, Xiamen, China. His research interests include modelling and control of converter systems and their applications to industry, transportation, and utilities.